Evolution of Quasiparticle Properties in UGe_2 with Hydrostatic Pressure Studied via the de Haas–van Alphen Effect

T. Terashima, T. Matsumoto, C. Terakura, and S. Uji
National Institute for Materials Science, Tsukuba, Ibaraki 305-0047, Japan

N. Kimura, M. Endo, T. Komatsubara, and H. Aoki
Center for Low Temperature Science, Tohoku University, Sendai, Miyagi 980-8578, Japan
(Received 2 May 2001; published 28 September 2001)

We report measurements of the de Haas–van Alphen effect in UGe_2 under hydrostatic pressures up to 17.6 kbar, exceeding the critical pressure P_c for the suppression of ferromagnetism. A discontinuous change of the Fermi surface is found to occur across P_c. Substantially enhanced effective masses ($\sim 40 m_e$) are found near P_c on both the ferromagnetic and the paramagnetic sides.

DOI: 10.1103/PhysRevLett.87.166401 PACS numbers: 71.18.+y, 71.27.+a, 74.70.Tx

Recently several magnetic heavy-fermion compounds have been shown to become superconducting as they are driven by hydrostatic pressure near quantum critical points (QCP's) where magnetic transition temperatures go to absolute zero [1–5]. Among them, UGe_2 [5] is of particular interest, in which the same heavy fermions seem to participate in both superconductivity (SC) and ferromagnetism. At ambient pressure, UGe_2 is ferromagnetic below the Curie temperature T_c of 52 K [6]. The low ratio of the ordered moment, $1.4\mu_B$/U, to the effective paramagnetic one, $\sim 2.7\mu_B$/U [6], is a clear sign of itinerant ferromagnetism. Strong magnetic anisotropy with the easy axis of magnetization along the crystallographic a axis is explained well by recent band-structure calculations including spin-orbit coupling [7]. With increasing pressure, T_c decreases and vanishes at the critical pressure $P_c \sim 16$ kbar [5,8–11]. Superconductivity is observed below 1 K in a limited pressure range, ~ 10–16 kbar, on the ferromagnetic side of the QCP [5,10,11].

Measurements of the electronic specific heat coefficient γ and the quadratic temperature coefficient of resistivity A, in the form $\rho = \rho_0 + AT^2$, indicate the existence of enhanced quasiparticle interactions in, at least, part of the pressure regime where the SC appears. The former γ, being ~ 30 mJ/mol K^2 at ambient pressure, increases steeply near 11 kbar and retains a large and nearly constant value of ~ 100 mJ/mol K^2 up to ~ 14 kbar (above which no data are currently available) [10]. The coefficient A has previously been reported to exhibit a clear peak near 12–13 kbar [5,9,10], though a recent report suggests that it remains large up to ~ 15 kbar [11]. The steep rises in γ and A near 11–12 kbar may be related to an anomaly that was found below T_c in the ferromagnetic phase. The anomaly shows up in the temperature derivative of resistivity as a broad peak [9–11], which defines a characteristic temperature T_x, and also a slight increase in the magnetization is observed below T_x at high pressures [11]. The characteristic temperature T_x, being ~ 30 K at ambient pressure, decreases with pressure, and appears to reach absolute zero at $P_x \sim 12$–13 kbar [9–11]. It has been proposed that the T_x anomaly may be due to a charge density wave (CDW) transition [5,11]. Band-structure calculations suggest that the major sheet of the majority-spin Fermi surface (FS) is quasi-two-dimensional (Q2D) and has a favorable shape for nesting [7,12]. However, there is no conclusive evidence of a CDW formation below T_x.

It is intriguing that the superconducting phase in UGe_2 is entirely enclosed in the ferromagnetic phase. Theoretical studies on SC mediated by magnetic fluctuations near a second-order ferromagnetic QCP indicate that SC can occur on both sides of the QCP [13]. Further, Ce-based antiferromagnetic heavy-fermion compounds exhibit SC on both sides of their QCP's [1–4]. In order to explain the absence of SC in the paramagnetic phase of UGe_2, it has been suggested that the ferromagnetic transition is first order near P_c and hence that the SC is mediated by magnetic fluctuations associated with the (hypothetical) second-order critical point at P_x rather than the one at P_c [5,11].

Any realistic models of the unparalleled SC in UGe_2 will obviously require detailed information on the evolution of electronic structure with pressure, which may most suitably and directly be studied via the de Haas–van Alphen (dHvA) effect. In this paper, we report dHvA effect measurements performed on UGe_2 under hydrostatic pressures up to 17.6 kbar, well exceeding P_c.

The UGe_2 single crystal used in the present study was grown by the Czochralski pulling method in a tetra-arc furnace. The residual resistivity ratios are 150 and 70 for currents along the a and b axes, respectively, indicating that the crystal is high quality. Hydrostatic pressures P up to 17.6 kbar were produced by a clamped piston-cylinder cell consisting of a NiCrAl alloy inner cylinder [14] and a BeCu outer shell with Daphne 7373 oil (Idemitsu Co. Ltd., Tokyo) as a pressure-transmitting medium. A manganin gauge was used to determine the pressure at low temperatures, the pressure coefficient of which was calibrated by measuring the superconducting transition of Sn in separate runs. The cell containing the

sample, a balanced pickup coil, and a manganin gauge was directly immersed into a ^{3}He-^{4}He mixture in a dilution refrigerator (base temperature ~30 mK) integrated with a 20 T superconducting magnet. dHvA oscillations were detected by measuring ac susceptibility, the magnetic field B applied parallel to the b axis, a hard axis of magnetization, within the accuracy of a few degrees. To minimize eddy-current heating of the cell/sample assembly, the frequency and amplitude of the ac excitation field mostly used were $f = 17$ Hz and $B_{ac} = 0.62$ mT. Further, for effective mass determination, amplitude data taken at temperatures T no less than 70 mK were analyzed. For these choices of f, B_{ac}, and T, eddy-current effects are negligible as was confirmed by an effective-mass determination using $B_{ac} = 0.21$ mT which yielded the identical effective mass as for $B_{ac} = 0.62$ mT.

We see three frequencies, α, β, and γ, in the spectrum for $P = 0$ bar (Fig. 1); $F_\alpha = 6800 \pm 30$ T, $F_\beta = 7710 \pm 10$ T, and $F_\gamma = 9130 \pm 30$ T. The orbit area associated with the strongest frequency β is 29% of the cross section of the Brillouin zone. Effective masses for the α, β, and γ orbits are determined from the temperature dependences of the oscillation amplitudes (see Fig. 2 for β) to be 23 ± 3, 12 ± 1, and 17 ± 2 in the units of the free electron mass m_e, respectively. We also resolved several smaller frequencies ($F < 1000$ T) by scanning wider field ranges, though we do not go into detail about them. While the present spectrum is in good agreement with the one recently reported [15], it is not very consistent with the previous ones [16], in which the strongest frequency was found at ~8200 T, and frequencies with fairly large amplitudes were observed near 6000 and 9000 T. The discrepancy may be due to a slight difference in the alignment of crystals.

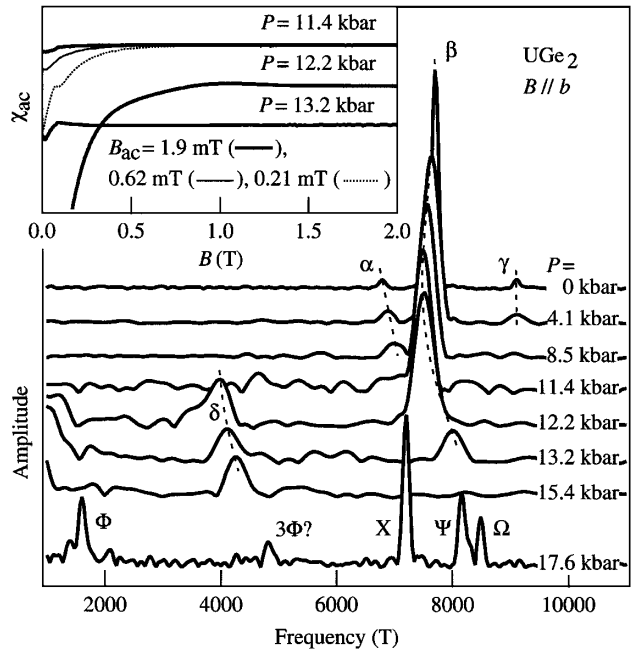

FIG. 1. Fourier spectra of dHvA oscillations as a function of pressure. Frequencies, or orbits, are labeled by Greek letters. Each spectrum is arbitrarily scaled for clarity. Inset: Superconducting diamagnetic signals observed in the ac susceptibility χ_{ac} measured with the excitation field B_{ac}.

The application of pressure up to 8.5 kbar brings only moderate changes in the FS (Figs. 1 and 3, the latter of which summarizes quasiparticle properties as functions of pressure). The pressure coefficients of dHvA frequencies $d \ln F/dP$ for $P \leq 8.5$ kbar are (3.9 ± 0.1) and $(-2.1 \pm 0.1) \times 10^{-3}$ kbar^{-1} for the α and β orbits, respectively, while the frequency γ is constant within experimental error up to 4.1 kbar and is not visible at 8.5 kbar, probably because of small amplitude. The effective mass for the β orbit is slightly enhanced to $(15 \pm 1)m_e$ at $P = 8.5$ kbar [Fig. 3(c)].

We have confirmed SC at the pressures of 11.4, 12.2, and 13.2 kbar (Fig. 1, inset). The diamagnetic signal is largely influenced (i.e., suppressed) by small ac excitation fields of less than ~2 mT and is strongest at 12.2 kbar.

In the pressure range from 11.4 to 15.4 kbar, appreciable changes are found in dHvA oscillations (Figs. 1 and 3). The frequency β reaches a minimum at 11.4 kbar, rapidly increases with the pressure coefficient of 64×10^{-3} kbar^{-1} between 12.2 and 13.2 kbar, and is not visible at 15.4 kbar. The amplitude of the oscillation is substantially damped in this pressure regime; the amplitude at 13.2 kbar is about 1/40 of that at 0 kbar or less [Fig. 3(b)]. The effective mass for β amounts to $(39 \pm 5)m_e$ at 13.2 kbar [Figs. 2 and 3(c)]. Further, a new frequency δ shows up at 12.2 kbar (Fig. 1), having the frequency of 4040 ± 40 T and the effective mass of $(22 \pm 9)m_e$. The frequency δ also rapidly increases with the pressure coefficient of $(15 \pm 4) \times 10^{-3}$ kbar^1 between 12.2 and 15.4 kbar.

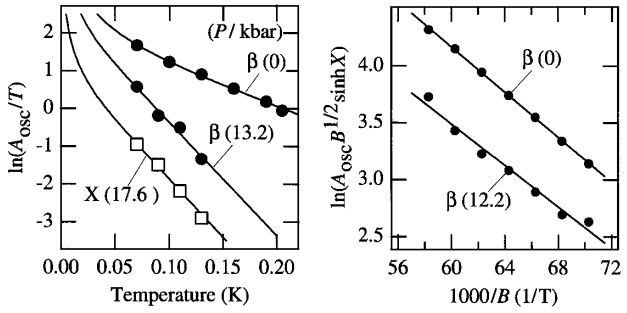

FIG. 2. Examples of temperature (left panel) and field (right panel) dependences of oscillation amplitudes A_{osc} (at constant field and temperature, respectively). Data sets are arbitrarily shifted with each other for clarity. Greek letters and values in parentheses give orbit names and measurement pressures, respectively, $X = -K(m^*/m_e)T/B$, and $K = 14.69$ T/K. Curves are fits to the theoretical formula $A_{osc}/T \sim \sinh^{-1} X$ and $\ln(A_{osc}B^{1/2} \sinh X) \sim -K(m^*/m_e)x/B$. These and other similar fits give estimates of the effective mass m^* and $(m^*/m_e)x$, with x being the Dingle temperature, as shown in Fig. 3.

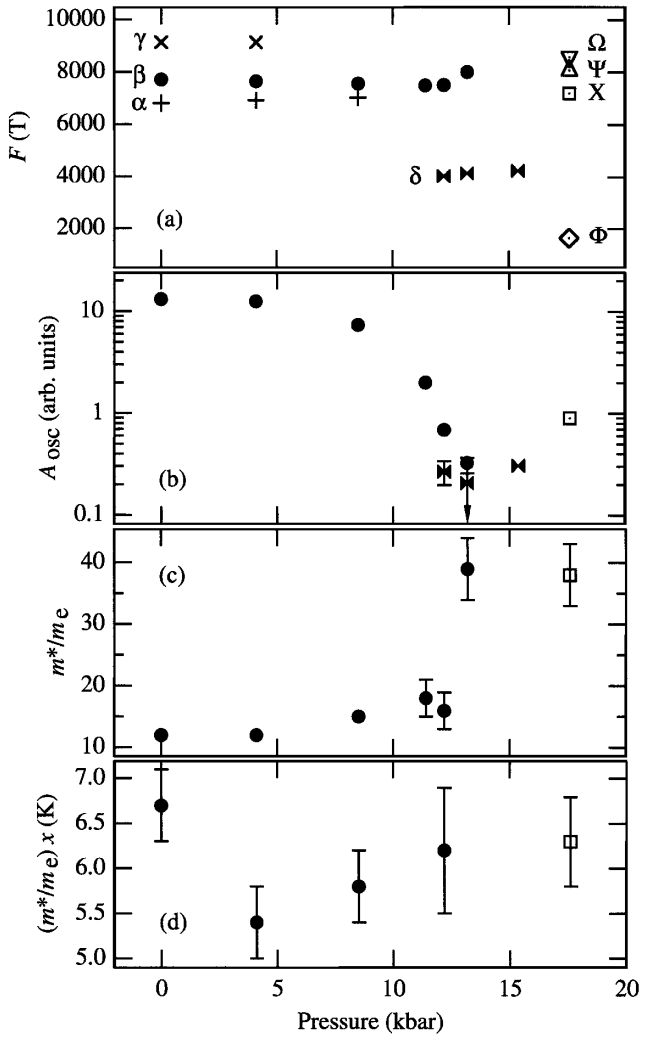

FIG. 3. Pressure variations of (a) frequencies, (b) oscillation amplitudes at $T = 0.07$ K and $B = 17.0$ T, (c) effective masses m^*, and (d) $(m^*/m_e)x$, with x being the Dingle temperature. The relation between symbols and orbits is given in (a). The latter three quantities are given for selected orbits and pressures. The error of each point is smaller than or comparable to a mark size unless an error bar is attached. In (b), the data points at 13.2 kbar show the amplitudes evaluated at $B = 19.1$ T and hence are regarded as upper limits to those at 17.0 T, as indicated by the arrow.

A discontinuous change of dHvA spectra occurs between 15.4 and 17.6 kbar (Fig. 1). We see four fundamental frequencies at 17.6 kbar; $F_\Phi = 1650 \pm 30$ T, $F_X = 7200 \pm 10$ T, $F_\Psi = 8180 \pm 30$ T, and $F_\Omega = 8490 \pm 40$ T. A peak near 4800 T may be another fundamental or the third harmonic of Φ. The effective masses for Φ, X, and Ψ are estimated to be 30 ± 6, 38 ± 5, and 39 ± 5 in the units of m_e (see Fig. 2 for X).

Based on the band-structure calculations [7,12,17], the frequency β is most probably attributed to an extremal orbit on the large Q2D majority-spin sheet of the FS. Its presence at ambient pressure does not seem compatible with the proposed CDW formation due to the nesting of the Q2D sheet at T_x; an energy gap opening on nested portions of the sheet would kill the frequency β. The calculations [17] further suggest that the frequency α may be attributed to another extremal orbit on the same sheet, while γ may arise from another large FS sheet with a hole character.

The frequency δ suddenly appears at 12.2 kbar (Fig. 1). However, this does not indicate such a radical change of band structure that a new band crosses the Fermi level to form a new FS pocket. It would inevitably accompany abrupt changes in dimensions of other FS sheets to conserve the total FS volume, which is not observed; the frequency β smoothly varies from 11.4 to 12.2 kbar. Therefore, the appearance of δ is attributed to pressure-induced continuous modification of the FS sheets that already exist at lower pressures. The band-structure calculations [17] show a number of extremal orbits on the theoretical FS for ambient pressure. However, none of those frequencies, even roughly, matches δ. In order to explain the orbit δ, we tentatively suggest that the large hole surface, to which the frequency γ may be attributed, shrinks with pressure and splits into pieces to have new extremal orbits. Note that a parallel argument concerning the conservation of the FS volume applies to the disappearance of the frequency β at 15.4 kbar, and hence that it is most likely ascribable to a diminished amplitude of β.

The pressure coefficients of the frequencies β and δ for $P > \sim 12$ kbar (64 and 15×10^{-3} kbar^{-1}) are 1 order of magnitude larger than those of α and β in the low pressure regime (3.9 and -2.1×10^{-3} kbar^{-1}). Large pressure coefficients of dHvA frequencies seem to be a general sign of the proximity to a magnetic instability. In the prototypal heavy fermion $CeRu_2Si_2$, for example, pressure coefficients as large as 80×10^{-3} kbar^{-1} are found [18]. For comparison, in $CeCo_2$, a "stable" paramagnet far away from a magnetic instability, the coefficients are 7×10^{-3} kbar^{-1} at most [19], and in a representative metal Cu the coefficient for the belly orbit is 0.4×10^{-3} kbar^{-1} [20].

The distinct dHvA spectra at 15.4 and 17.6 kbar indicate that the FS abruptly changes across $P_c \sim 16$ kbar. This is not trivial. In the spirit of a Doniach phase diagram [21], a QCP in Ce-based heavy fermions may be regarded as the point where $4f$ electrons change their nature from localized to itinerant. However, $5f$ electrons in UGe_2 are already itinerant at ambient pressure. Then, if P_c is a second-order QCP, a naive expectation may be that, as we approach P_c, the exchange splitting of the FS continuously reduces and hence that majority- and minority-spin FS in the ferromagnetic state gradually merge into spin-degenerate FS in the paramagnetic state. However, we did not see a minority-spin counterpart of the majority-spin frequency β (Fig. 1). Further, the frequency β does not even decrease as P_c is approached.

Huxley *et al.* [22] previously found a metamagnetic transition at pressures higher than P_c for the magnetic field

parallel to the easy axis and argued that the ferromagnetic transition changed from second order at low pressures to first order at some pressure below P_c [23]. The argument is based on a theory of itinerant electron metamagnetism, which deals with weakly or nearly ferromagnetic compounds [24]. It predicts that the ground state sensitively depends on the shape of the paramagnetic density of states (DOS) near the Fermi level. Namely, as pressure modifies the DOS, the ferromagnetic transition at T_c in a weakly ferromagnetic compound changes from second order to first order, and then the compound becomes a paramagnet that exhibits a metamagnetic transition in magnetic fields.

If the ferromagnetic transition is first order at pressures near P_c the sudden change of the dHvA spectra across P_c can readily be understood. Since the ferromagnetic and paramagnetic phases near P_c are separated by a first-order phase boundary, the FS discontinuously changes as the boundary is crossed. The first-order ferromagnetic transition near P_c would place fairly strong constraints on microscopic models of the SC. First, the exchange splitting cannot be assumed vanishingly small in the pressure regime where the SC is observed. Second, critical magnetic fluctuations associated with a second-order QCP do not exist in UGe_2 near P_c.

The effective mass for the orbit β gradually increases till 12.2 kbar, then steeply rises to about 3 times as large a value as the ambient-pressure value [Fig. 3(c)]. This is consistent with the behavior of the electronic specific heat coefficient γ [10], mentioned earlier. Although γ was determined only up to $\sim$14 kbar, the present result that the orbits X, Ψ, and Ω observed at 17.6 kbar are similar to the orbit β at 13.2 kbar in dimensions and effective masses strongly suggests that γ at 17.6 kbar is comparable to values found between $\sim$12 and $\sim$14 kbar. That is, quasiparticle masses are enhanced near P_c on both the ferromagnetic and paramagnetic sides. This is in sharp contrast with what the peak of A near 12–13 kbar suggests [5,9,10]. We also note that it remains an open question if quasiparticle interactions leading to the observed mass enhancement near P_c may relate to the mechanism of the SC; the SC in our sample starts at 11.4 kbar, and becomes strongest at 12.2 kbar (Fig. 1, inset), while the substantial mass enhancement is not observed until 13.2 kbar.

Lastly, we point out that the origin of the pronounced reduction of the oscillation amplitude of β for $P > \sim$11 kbar [Fig. 3(b)] is not clear. The ratio of the amplitudes at 0 and 12.2 kbar is $\sim 1/20$ at $T = 0.07$ K and $B = 17$ T. This cannot be accounted for by the temperature and Dingle reduction factors with the values of m^* and $(m^*/m_e)x$ shown in Fig. 3; even if we assume the maximum error in the parameters, the reduction is 50% at most. With the standard Lifshitz-Kosevich theory [25], it then follows that the curvature factor, which reflects the local shape of the FS near an extremal orbit, is at least $\sim$100 times larger at 12.2 kbar than at 0 kbar. However, since the frequency β changes only by $\sim$2% from 0 to 12.2 kbar [Fig. 3(a)], substantial deformation of the Q2D sheet that is necessary for the large change in the curvature factor is not very likely to take place in this pressure span.

Work at Tohoku University was supported by a Grant-in-Aid for Scientific Research of MEXT Japan.

[1] D. Jaccard, K. Behnia, and J. Sierro, Phys. Lett. A **163**, 475 (1992).
[2] R. Movshovich *et al.,* Phys. Rev. B **53**, 8241 (1996).
[3] F. M. Grosche *et al.,* Physica (Amsterdam) **223B/224B**, 50 (1996).
[4] I. R. Walker *et al.,* Physica (Amsterdam) **282C–287C**, 303 (1997).
[5] S. S. Saxena *et al.,* Nature (London) **406**, 587 (2000).
[6] A. Menovsky *et al., High Field Magnetism* (North-Holland, Amsterdam, 1983), p. 189.
[7] A. B. Shick and W. E. Pickett, Phys. Rev. Lett. **86**, 300 (2001).
[8] K. Nishimura *et al.,* J. Alloys Compd. **213/214**, 383 (1994).
[9] G. Oomi, T. Kagayama, and Y. Onuki, J. Alloys Compd. **271–273**, 482 (1998).
[10] N. Tateiwa *et al.,* J. Phys. Condens. Matter **13**, L17 (2001).
[11] A. Huxley *et al.,* Phys. Rev. B **63**, 144519 (2001).
[12] H. Yamagami and A. Hasegawa, Physica (Amsterdam) **186B–188B**, 182 (1993).
[13] D. Fay and J. Appel, Phys. Rev. B **22**, 3173 (1980); R. Roussev and A. J. Millis, Phys. Rev. B **63**, 140504(R) (2001).
[14] The NiCrAl alloy was produced in house at the National Institute for Materials Science under the supervision of one of the authors, T. M.
[15] R. Settai *et al.,* Meeting Abstracts of the Physical Society of Japan **55**, 468 (2000).
[16] Y. Onuki *et al.,* J. Phys. Soc. Jpn. **60**, 2127 (1991); K. Satoh *et al.,* J. Phys. Soc. Jpn. **61**, 1827 (1992).
[17] S. Tejima, H. Yamagami, and N. Hamada (unpublished).
[18] M. Takashita *et al.,* J. Magn. Magn. Mater. **177–181**, 417 (1998); H. Aoki *et al.,* J. Phys. Soc. Jpn. **70**, 774 (2001).
[19] M. Takashita *et al.,* Physica (Amsterdam) **281B/282B**, 738 (2000).
[20] I. M. Templeton, Can. J. Phys. **52**, 1628 (1974).
[21] S. Doniach, Physica (Amsterdam) **91B**, 231 (1977).
[22] A. Huxley, I. Sheikin, and D. Braithwaite, Physica (Amsterdam) **284B–288B**, 1277 (2000).
[23] In the present measurements the magnetic field was applied parallel to a hard axis of magnetization and hence metamagnetic transitions did not occur up to the highest magnetic fields applied.
[24] T. Moriya, J. Phys. Soc. Jpn. **55**, 357 (1986); H. Yamada, Phys. Rev. B **47**, 11 211 (1993).
[25] D. Schoenberg, *Magnetic Oscillations in Metals* (Cambridge University Press, Cambridge, 1984).